


***Ab initio* study of temperature- and laser-induced phase transitions in TiO₂**Sergej Krylow  and Martin E. Garcia*Theoretical Physics and Center for Interdisciplinary Nanostructure Science and Technology (CINSAT), University of Kassel, Heinrich-Plett-Strasse 40, 34132 Kassel, Germany*

(Received 25 September 2019; published 3 December 2019)

We analyze the bulk phase transitions of the three titanium dioxide polymorphs anatase, rutile, and brookite in thermodynamical equilibrium and after ultrafast laser excitation using the generalized solid-state nudged elastic band (G-SSNEB) method. For calculating the forces and stresses needed for G-SSNEB, we use electronic-temperature dependent density functional theory calculations. Our results show that the anatase-rutile and brookite-rutile phase transitions have a considerably lower energy barrier than the anatase-brookite phase transition in the thermodynamical equilibrium and upon laser excitation. The obtained transition temperatures in thermodynamical equilibrium are consistent with experimentally observed ones. Furthermore, our calculations show that the pathways of the phase transition are not affected considerably by the applied laser pulse. Although the pathways do not change considerably we see that the rutile phase is stabilized by the laser pulse.

DOI: [10.1103/PhysRevB.100.224101](https://doi.org/10.1103/PhysRevB.100.224101)**I. INTRODUCTION**

Titanium dioxide nanoparticles show an extraordinary high photocatalytic activity due to their high surface area [1] compared to the volume of the sample. This property makes titanium dioxide an ideal candidate for various technical applications, like the electrolysis of water [2,3], air purification [4,5], and water treatment [6,7]. The best photocatalytic activity is usually achieved by mixtures of the three main titanium dioxide polymorphs, rutile, anatase, and brookite [8–11]. However, a degradation of the photocatalytic activity can occur in time due to phase transitions between these three polymorphs, especially in the high temperature regime. Naturally, much effort was put into the analysis of the phase transitions between these three polymorphs. It was found that their stability is very sensitive to the particle size and temperature. In particular, rutile becomes the most stable polymorph for particle sizes above 15 to 35 nm [12–14]. Brookite, on the other hand, becomes the most stable polymorph in the range of approximately 11 to 35 nm, and for even smaller particle sizes anatase becomes the most energetically stable polymorph [13,14]. This behavior is attributed to the size- and polymorph-dependent surface energy [15]. The critical temperatures for the occurrence of anatase-rutile and brookite-rutile phase transitions are known to be 600 and 700 K, respectively [16]. The anatase-brookite phase transition, on the other hand, cannot be driven thermally if no brookite nucleus is initially present in the sample [17]. It was also reported that the phase transition between anatase and rutile can also be driven by a femtosecond laser pulse [18,19]. However, little is known about the detailed energy pathways during the phase transitions.

In this paper we analyze, on the basis of density functional theory calculations, the phase transition pathways of bulk rutile, anatase, and brookite in thermal equilibrium and upon ultrafast laser excitation. The structures of rutile, anatase, and brookite are shown in Fig. 1. We focus on bulk material

in order to avoid the treatment of surface effects, which would make the treatment complicated and unclear. To find optimized energy pathways we use the generalized solid-state nudged elastic band method (G-SSNEB) [20], modified by the climbing image technique [21]. The G-SSNEB method was already used by Vu *et al.* in Ref. [22] to analyze the anatase-rutile phase transitions. However, our calculations show an energy barrier for the anatase-rutile phase transition, which is about 5 times smaller than the one reported in Ref. [22]. We also obtain a low energy barrier for the brookite-rutile phase transition, which is comparable to the one between anatase and rutile. Furthermore, our results suggest a significantly higher energy barrier between anatase and brookite. This is consistent with experimental results, which suggest that the anatase-brookite phase transition cannot be thermally driven. Furthermore, we analyze the influence of ultrafast laser excitations on the different phases. We find that rutile becomes more stable, compared to anatase and brookite, after laser excitation. The transition pathways, however, stay nearly unaffected by the laser excitation.

The paper is organized as follows. In Secs. II A and II B we will give details on the G-SSNEB method and on our *ab initio* calculations, respectively. Then we discuss our results in Sec. III and conclude our work in Sec. IV.

II. METHODS**A. Generalized solid-state nudged elastic-band method**

To find the minimal energy pathway (MEP) between the titanium dioxide polymorphs, rutile, anatase, and brookite, we use the generalized solid-state nudged elastic-band method (G-SSNEB) developed by the group of Henkelmann *et al.* in Ref. [20]. The general idea of the G-SSNEB method is to connect two structures by a chain of transition structures, which are connected with springs [23]. Furthermore, it takes into account not only the atomic positions as a degree of

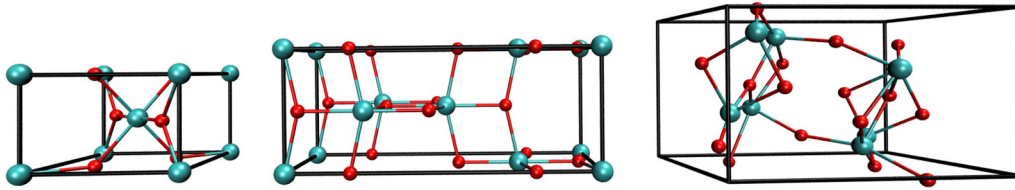


FIG. 1. Structures of the titanium dioxide polymorphs rutile (left), anatase (middle), and brookite (right). Titanium atoms are shown in cyan and oxygen atoms are shown in red.

freedom but also the lattice parameters. The forces and stresses for the G-SSNEB method are obtained from density functional theory calculations, which will be described in more detail in Sec. II B. The forces and stresses are then used to optimize the MEP with the G-SSNEB method using the fast inertial relaxation engine (FIRE) algorithm [24]. Finally, we employ the climbing image technique to obtain not only the MEB but also its maximum [21].

Before starting the calculations with the G-SSNEB method one has to define a mapping between the atoms of the two structures one is interested in. Figure 2 shows a schematic mapping between a structure A and a structure B. For each atom i of structure A one needs to define an atomic position r_j of atom j in structure B to which atom i will move during the phase transition. This defines a bijective mapping between the atoms in structure A and the ones in structure B. In general, most mappings would result in high energy pathways because either atoms would come very close to each other or many atomic bonds are broken. Thus, one has to put particular care into the modeling of the mapping. During the construction of the mapping we have focused on minimizing the number of broken bonds and maximizing the distances between atoms during the phase transition. Furthermore, one can employ similarities between the titanium dioxide polymorphs, i.e., the x - y symmetry of rutile and anatase. By using the above considerations we have generated the mappings between the titanium dioxide polymorphs [25]. After the generation of the mapping we use a linear interpolation in order to obtain the initial MEP on which we apply the G-SSNEB method. Note, that neither the mapping nor the optimized MEP have to be ideal. Furthermore, for larger supercells more mappings

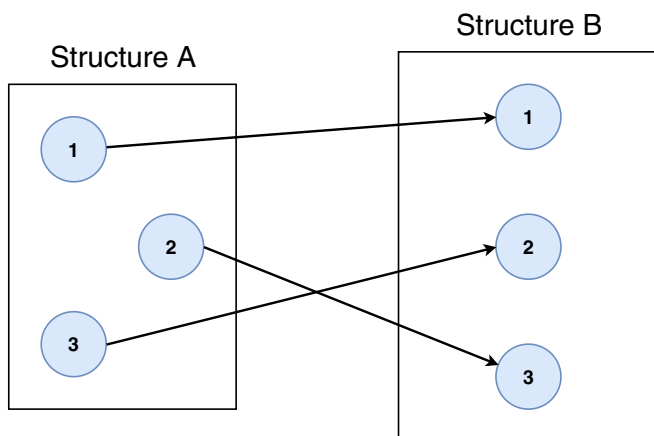


FIG. 2. Schematic mapping between the atoms of two structures.

are possible, which might be energetically more favorable. However, larger supercells are computationally much more expensive and therefore are not considered in this work. Our calculations provide, therefore, an upper bound for the energy barrier of the phase transitions in the analyzed titanium dioxide polymorphs.

B. Density functional theory calculations

For the calculation of the forces and stresses we use our in-house Code for Highly excIted Valence Electron Systems (CHIVES) which is an electronic-temperature-dependent density functional theory (DFT) code [26]. It is based on atom-centered Gaussian basis sets, the local density approximation, and relativistic pseudopotentials. We have previously used CHIVES to simulate the structural response of silicon [27,28], antimony [29], graphene [30], and titanium dioxide [26] immediately after femtosecond-laser excitation. For the calculation of the bulk properties of the titanium dioxide polymorphs we use periodic boundary conditions, a supercell with 48 atoms and a $2 \times 2 \times 2$ k grid. Note, that the energies, lattice parameters, and atomic positions do not change considerably for larger supercells. To calculate strains and stresses we use the described technique in Ref. [31]. To model titanium dioxide after laser excitation we use the fact that the intraband relaxation in anatase and rutile is finished within about 20 fs [32]. The interband relaxation, on the other hand, takes several picoseconds to finish [32]. We assume that this is also the case for brookite. After the intraband relaxation is finished the system can be described with two chemical potentials, one for the valence band and another one for the conduction band as was done previously in Refs. [33,34] for rutile and tellurium. The two chemical potentials define two Fermi Dirac distributions with which the electronic states are occupied. We set the percentage of excited valence electrons to 0.2% and 0.5%, respectively. In general, the two Fermi Dirac distributions correspond to two different electronic temperatures. In our work we assume that both electronic temperatures are equal and we set these to 300 K. By changing the percentage of excited electrons we modify the potential energy surface (PES), which will affect the MEP.

III. RESULTS

A. Structure optimization

We have first optimized the energy with respect to the atomic positions and the lattice parameters of the three structures corresponding to the analyzed polymorphs. The atomic positions were optimized using the FIRE algorithm [24]. The

TABLE I. Optimized lattice parameters and total energies of rutile, anatase, and brookite.

	N_{unitcell}	a (nm)	b (nm)	c (nm)	E (eV/atom)
Rutile	6	0.4557	0.4557	0.2931	-820.15268
Anatase	12	0.3745	0.3745	0.9535	-820.15513
Brookite	24	0.9121	0.5406	0.5091	-820.15867

lattice parameters were optimized by repeatedly calculating the strains and changing the lattice parameters accordingly until convergence is achieved. Table I shows the optimized lattice parameters a , b , c , and the total energies for each unit cell of the three polymorphs analyzed in this paper. Note, that the lattice parameter may vary by about 2% in rutile, depending on the used exchange-correlation approximation [35]. We assume that this is also the case for anatase and brookite. Therefore, the obtained lattice parameters are consistent with the ones from other publications [16,36]. Furthermore, one can see that the total energies of the titanium dioxide polymorphs are nearly equal. This contradicts experimental results, for which rutile was observed to be the most stable polymorph for bulk material. However, it is still unknown quantitatively how large the energetic differences between the polymorphs are because these depend crucially on particles size, particle morphology, and ambient conditions. Theoretically, one can modify the energy relation between the polymorphs by using different exchange and correlation functionals in the DFT calculations [22,37]. Since the correct energy relation between the polymorphs is unknown, we do not include any correction to the energies.

B. Minimal energy pathways in thermal equilibrium

After generating the initial MEP, as described in Sec. II A, we have used the G-SSNEB method to calculate the optimized phase transition pathways. The MEP is considered converged if the change of the energy is less than 2.7×10^{-3} eV summed over all transition structures of the MEP. In case of the brookite-rutile and anatase-brookite phase transitions the convergence criterium was not fulfilled during our calculations. However, each obtained pathway represents a possible phase transition pathway even though no convergence is achieved. This is true because the transition structures along the pathway, obtained by the G-SSNEB method, are always approximately equidistant from each other in an abstract sense. Since real life materials have a smooth potential energy surface, one can expect that no steplike behavior of the potential energy surface occurs. Thus, also the obtained pathway at each time step of the G-SSNEB method can be considered to be smooth and therefore a possible transition pathway. The optimization of the pathway merely finds an even lower energy barrier or a somewhat different pathway. The dominant factor in the quality of a phase transition pathway is therefore not the convergence but the energy barrier, i.e., a converged pathway with a high energy barrier is worse than a nonconverged pathway with a low energy barrier. In order to obtain representative MEPs for the brookite-rutile and anatase-brookite phase transitions we use the following

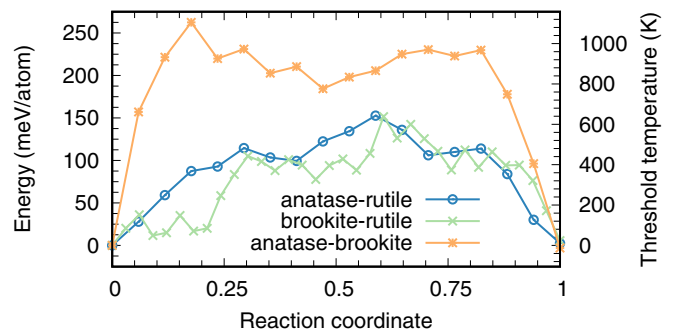


FIG. 3. Energy along the calculated MEP between anatase-rutile (stars), brookite-rutile (crosses), and anatase-brookite (circles) in the thermal equilibrium. The first named polymorph corresponds to 0 and the second named polymorph corresponds to 1 on the reaction coordinate. The energies are offset by the energy of the first named polymorph.

protocol. We have firstly optimized the atomic positions for 1500 steps. Then we have included the degrees of freedom of the lattice parameters and performed another 100 optimization steps. In these calculations we did not use the climbing image technique because it is only applicable when the current MEP is close to the converged one [21]. At the end of the optimization the change of the energy is 0.19 and 0.07 eV for the brookite-rutile and anatase-brookite phase transitions, respectively. The energy along the obtained MEP is shown in Fig. 3 for the anatase-rutile (blue circles), brookite-rutile (green crosses), and anatase-brookite (orange stars) phase transitions [38]. The MEPs are offset by the energy of the starting structures, which are always named first, i.e., anatase for the anatase-rutile phase transition. A value of 0 for the reaction coordinate corresponds to the starting structure and a value of 1 to the final structure. For the anatase-rutile phase transition one can see that the evolution of the MEP shows a nearly monotonic increase until the highest energy structure at about 0.6 and a monotonic decrease afterwards. The energy difference between anatase and the highest energy structure along the MEP is 152.66 meV/atom. Approximately the same value is obtained for the energy difference between rutile and the highest energy structure. The obtained energy barrier for the thermal equilibrium is about a factor 5 smaller than in Ref. [22]. This discrepancy might be attributed to a better initial mapping in our work. The brookite-rutile phase transition shows a similar evolution of the MEP. However, since it did not converge it shows a more fluctuating behavior. Note, that the obtained MEP and the obtained energies along the pathway are an upper bound for the phase transition. The obtained energy difference between the structure with the highest energy along the MEP compared to brookite and rutile is 152.66 and 145.85 meV/atom, respectively. Contrary to the two previously described phase transitions, the anatase-brookite phase transition has a considerably higher energy barrier. Figure 3 shows that the energy of the transition structures rises fast and stays flat for the biggest part of the MEP. The obtained energy difference between the highest energy structure along the MEP compared to anatase and brookite is 262.59 and 265.58 meV/atom, respectively.

We also show the threshold temperatures T for the occurrence of the phase transitions in Fig. 3, which are calculated using

$$E_{\text{kin}} = \frac{1}{2} \sum_{i=1}^N m_i |\vec{v}_i|^2 = \frac{3}{2} N k_B T. \quad (1)$$

Here the sum goes over all atoms i , m_i is the mass of the i th atom, \vec{v}_i is the velocity, and k_B is the Boltzmann constant. Note, that the potential energy, obtained in the G-SSNEB calculations, and the kinetic energy are equal in an equilibrated system. For the anatase-rutile phase transition we obtain a threshold temperature of about 600 K, which is comparable to experimentally observed ones, which generally lie in the region between 500 and 700 K [14,39–43]. For the brookite-rutile phase transition we obtain a threshold temperature of about 600 K, which also matches the observed temperature in the experiment of above 650 K [17]. From our calculations we see that the anatase-brookite phase transition has a high threshold temperature. Our results also show that for increasing temperatures anatase and brookite will transform to rutile before the anatase-brookite phase transition can take place. This is consistent with experimental results because the anatase-brookite phase transition can only be observed experimentally when the analyzed sample already contains brookite particles [17].

Our results suggest reversible phase transitions for all three analyzed polymorphs. This contradicts experimental observations, which indicate that the anatase-rutile phase transition is irreversible [44,45]. There are several possibilities to explain this discrepancy. A major difference between our calculations and experiments is that we focus on bulk material, whereas experiments were performed on nanoparticles. Thus, morphology and grain size become relevant. Note, that stability of titanium dioxide polymorphs depends on the surface energy [13]. Another important source of discrepancy is the temperature driven mobility of the nanoparticles. The increased mobility leads to an aggregation of particles and therefore favors the generation of rutile. The experimentally reported phase transition temperature is therefore a convolution of interacting properties. In our simulation we do not take the problem of the morphology, particle mobility, or grain size into account. Furthermore, there are two additional reasons why phase transitions are irreversible. First, the obtained phase transitions correspond to a collective transformation of the whole bulk material. This is unlikely to occur in real systems undergoing first order phase transitions. In general, the transition rather proceeds through nucleation starting from small clusters. Second, rutile should be the most stable polymorph for bulk material [13]. In our calculations all three polymorphs have approximately the same energy. Although the correct energy relation between the polymorphs is unknown, a lower energy for rutile would support the claim that the phase transitions are irreversible. In that case it could be possible that at a certain temperature anatase or brookite transform to rutile but the back transformation at the same temperature is not possible.

Based on the analysis of the atomic pathways we can confirm that the phase transitions are reconstructive, i.e., bonds are broken during the phase transition. This was also claimed in Ref. [16] for the anatase-rutile phase transition.

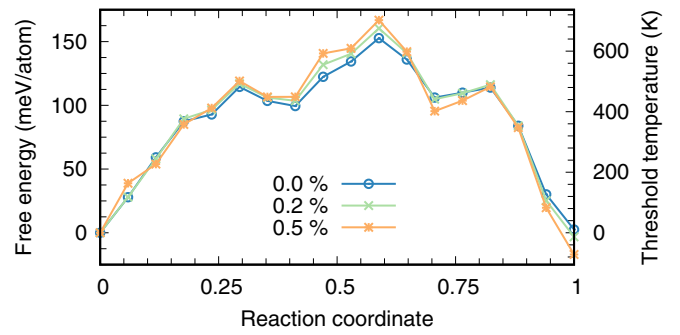


FIG. 4. Free energy along the calculated MEP for the anatase-rutile phase transition in the thermal equilibrium (circles) and the excited cases with 0.2 (crosses) and 0.5% (stars) of excited valence electrons. Anatase corresponds to 0 and rutile corresponds to 1 on the reaction coordinate. The free energies are offset by the energy of anatase at the corresponding excitation.

Furthermore, we can calculate the number of broken bonds during the phase transitions. We consider a bond to be broken if the distance between the bonded atoms exceeds a value of 0.233 nm. Note, that for the analyzed titanium dioxide polymorphs all bond distances lie in the region between 0.185 and 0.206 nm. Thus, the chosen criterium is reasonable to distinguish the broken bonds between the starting and final structure in our calculations. For our supercell with 48 atoms we obtain that 32 bonds are broken during the anatase-rutile phase transition, 28 bonds during the brookite-rutile phase transition, and 32 bonds during the anatase-brookite phase transition.

C. Minimal energy pathways in laser excited TiO_2

Additionally to the analysis at the thermal equilibrium we analyze the behavior of the phase transitions after laser excitation by setting the percentage of excited valence electrons to 0.2% and 0.5%, respectively. In the excited case we have to consider the free energy of the system [26]. However, in our calculations we only include the electronic contribution to the free energy and neglect the contribution from the ions.

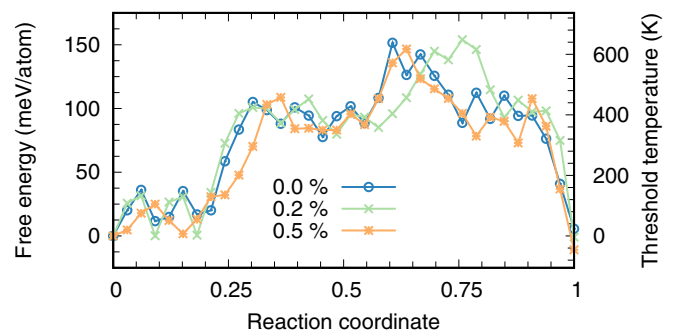


FIG. 5. Free energy along the calculated MEP for the brookite-rutile phase transition in the thermal equilibrium (circles) and the excited cases with 0.2 (crosses) and 0.5% (stars) of excited valence electrons. Brookite corresponds to 0 and rutile corresponds to 1 on the reaction coordinate. The free energies are offset by the energy of brookite at the corresponding excitation.

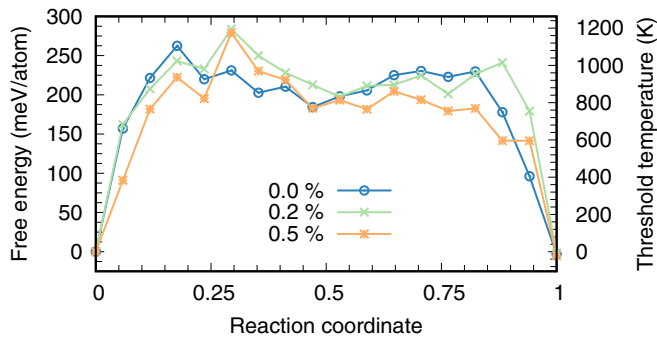


FIG. 6. Free energy along the calculated MEP for the anatase-brookite phase transition in the thermal equilibrium (circles) and the excited cases with 0.2 (crosses) and 0.5% (stars) of excited valence electrons. Anatase corresponds to 0 and brookite corresponds to 1 on the reaction coordinate. The free energies are offset by the energy of anatase at the corresponding excitation.

The calculation of the free energy of the ions is not possible because the transition structures are not in equilibrium and do not have a defined free energy. The starting and final structure, used in the calculation of the MEPs in the excited case, were optimized with respect to the atomic positions. The optimization of the lattice parameters were neglected. With this we model the pathway directly after laser excitation for which the lattice did not yet change. Furthermore, we use the MEP calculated for the thermal equilibrium as a starting point to reduce the computational cost of the MEP optimization. Similar to the thermal equilibrium calculations only the anatase-rutile MEP did converge for the used energy convergence criterium of 2.7×10^{-3} eV. For the other phase transitions we have used a similar protocol as before. First, we have performed 500 optimization steps using only the atomic degrees of freedom and then another 100 optimization steps with the cell degrees of freedom included. Figure 4 shows the free energy along the obtained MEP for the anatase-rutile phase transition in the thermal equilibrium and the excited cases. One can see that the energy of the highest energy structure is slightly increasing with respect to anatase and rutile for higher excitations. Furthermore, rutile becomes more stable compared to anatase in the excited case. Thus,

the laser excitation favors and stabilizes rutile. The brookite-rutile and anatase-brookite phase transitions, shown in Figs. 5 and 6, show larger changes of the energies along the MEP. These are probably due to the fact that the MEP did not converge completely. The energy barriers of both phase transitions stay nearly unaffected by the laser pulse. In the case of the brookite-rutile phase transition one can see that rutile becomes more stable than brookite with higher excitation. For the anatase-brookite phase transition brookite becomes slightly more stable. In addition to the change of the PES, the laser pulse also heats the system through electron-phonon coupling. From the above results we can conclude that the heating of the material due to electron-phonon coupling will mainly drive the phase transitions.

IV. CONCLUSION

In conclusion, we have calculated the energy barriers and threshold temperatures of the anatase-rutile, brookite-rutile, and anatase-brookite phase transitions. In particular, we show that the anatase-rutile and brookite-rutile phase transitions are energetically more favorable than the anatase-brookite phase transition. Furthermore, we can confirm that the phase transitions are reconstructive, i.e., bonds break during the phase transition. For the used supercells we obtain that 32 bond are broken during the anatase-rutile and anatase-brookite phase transitions, and 28 bond during the brookite-rutile phase transition. The MEPs do not change significantly after applying an ultrafast laser pulse. However, our results show that rutile becomes more stable with regards to anatase and brookite after laser excitation. The next step of the analysis is clearly to extend our calculations into the nanoparticle regime. Since in that case *ab initio* simulations become unfeasible, an analysis using classical, high-accuracy potentials might be preferable.

ACKNOWLEDGMENTS

Calculations for this research were conducted on the Lichtenberg high performance computer of the TU Darmstadt. S.K. gratefully acknowledges the financial support from the Otto-Braun-Fonds and the DFG project GA 465/18-1. Visualization of the structures were done with VMD [46].

- [1] X. Chen and S. S. Mao, *Chem. Rev.* **107**, 2891 (2007).
- [2] K. Fujihara, T. Ohno, and M. Matsumura, *J. Chem. Soc. Faraday Trans.* **94**, 3705 (1998).
- [3] A. L. Linsebigler, G. Lu, and J. T. Yates, *Chem. Rev.* **95**, 735 (1995).
- [4] A. Fujishima, X. Zhang, and D. A. Tryk, *Surf. Sci. Rep.* **63**, 515 (2008).
- [5] D. S. Muggli and L. Ding, *Appl. Catal. B* **32**, 181 (2001).
- [6] R. W. Matthews, *J. Phys. Chem.* **91**, 3328 (1987).
- [7] R. L. Pozzo, M. A. Baltanás, and A. E. Cassano, *Catal. Today* **39**, 219 (1997).
- [8] T. Ohno, K. Sarukawa, and M. Matsumura, *J. Phys. Chem. B* **105**, 2417 (2001).
- [9] R. Bacsa and J. Kiwi, *Appl. Catal. B* **16**, 19 (1998).
- [10] Q. Zhang, L. Gao, and J. Guo, *Appl. Catal. B* **26**, 207 (2000).
- [11] D. C. Hurum, K. A. Gray, T. Rajh, and M. C. Thurnauer, *J. Phys. Chem. B* **109**, 977 (2005).
- [12] Y. Hu, H.-L. Tsai, and C.-L. Huang, *Mater. Sci. Eng. A* **344**, 209 (2003).
- [13] H. Zhang and J. F. Banfield, *J. Mater. Chem.* **8**, 2073 (1998).
- [14] K.-R. Zhu, M.-S. Zhang, J.-M. Hong, and Z. Yin, *Mater. Sci. Eng. A* **403**, 87 (2005).
- [15] H. Zhang and J. F. Banfield, *J. Phys. Chem. B* **104**, 3481 (2000).
- [16] D. A. H. Hanaor and C. C. Sorrell, *J. Mater. Sci.* **46**, 855 (2011).
- [17] T. A. Kandiel, L. Robben, A. Alkaim, and D. Bahnemann, *Photochem. Photobiol. Sci.* **12**, 602 (2013).
- [18] J. Yang, H. Ma, G. Ma, B. Lu, and H. Ma, *Appl. Phys. A* **88**, 801 (2007).

- [19] P. Russo, R. Liang, R. X. He, and Y. N. Zhou, *Nanoscale* **9**, 6167 (2017).
- [20] D. Sheppard, P. Xiao, W. Chemelewski, D. D. Johnson, and G. Henkelman, *J. Chem. Phys.* **136**, 074103 (2012).
- [21] G. Henkelman, B. P. Uberuaga, and H. Jónsson, *J. Chem. Phys.* **113**, 9901 (2000).
- [22] N. H. Vu, H. V. Le, T. M. Cao, V. V. Pham, H. M. Le, and D. Nguyen-Manh, *J. Phys.: Condens. Matter* **24**, 405501 (2012).
- [23] See Supplemental Material at <http://link.aps.org/supplemental/10.1103/PhysRevB.100.224101> for a more detailed description of the G-SSNEB method.
- [24] E. Bitzek, P. Koskinen, F. Gähler, M. Moseler, and P. Gumbsch, *Phys. Rev. Lett.* **97**, 170201 (2006).
- [25] See Supplemental Material at <http://link.aps.org/supplemental/10.1103/PhysRevB.100.224101> for the used mappings between the three titanium dioxide polymorphs rutile, anatase, and brookite. Note, that the positions are given in atomic units.
- [26] E. S. Zijlstra, T. Zier, B. Bauerhenne, S. Krylow, P. M. Geiger, and M. E. Garcia, *Appl. Phys. A* **114**, 1 (2014).
- [27] T. Zier, E. S. Zijlstra, and M. E. Garcia, *Appl. Phys. A* **117**, 1 (2014).
- [28] T. Zier, E. S. Zijlstra, and M. E. Garcia, *Phys. Rev. Lett.* **116**, 153901 (2016).
- [29] S. Krylow, E. S. Zijlstra, F. C. Kabeer, T. Zier, B. Bauerhenne, and M. E. Garcia, *Phys. Rev. Mater.* **1**, 073601 (2017).
- [30] S. Krylow and M. E. Garcia, *EPJ Web Conf.* **205**, 05006 (2019).
- [31] Y. Le Page and P. Saxe, *Phys. Rev. B* **63**, 174103 (2001).
- [32] V. P. Zhukov and E. V. Chulkov, *J. Phys.: Condens. Matter* **22**, 435802 (2010).
- [33] E. M. Bothschafter, A. Paarmann, E. S. Zijlstra, N. Karpowicz, M. E. Garcia, R. Kienberger, and R. Ernstorfer, *Phys. Rev. Lett.* **110**, 067402 (2013).
- [34] P. Tangney and S. Fahy, *Phys. Rev. B* **65**, 054302 (2002).
- [35] B. Montanari and N. Harrison, *Chem. Phys. Lett.* **364**, 528 (2002).
- [36] S.-D. Mo and W. Y. Ching, *Phys. Rev. B* **51**, 13023 (1995).
- [37] Z.-H. Cui, F. Wu, and H. Jiang, *Phys. Chem. Chem. Phys.* **18**, 29914 (2016).
- [38] See Supplemental Material at <http://link.aps.org/supplemental/10.1103/PhysRevB.100.224101> for the complete atomic positions during the analyzed phase transitions. Note, that the positions are given in atomic units.
- [39] K. Okada, N. Yamamoto, Y. Kameshima, A. Yasumori, and K. J. D. MacKenzie, *J. Am. Ceram. Soc.* **84**, 1591 (2001).
- [40] J. Ovenstone and K. Yanagisawa, *Chem. Mater.* **11**, 2770 (1999).
- [41] J. Arbiol, J. Cerdà, G. Dezanneau, A. Cirera, F. Peiró, A. Cornet, and J. R. Morante, *J. Appl. Phys.* **92**, 853 (2002).
- [42] C. Byrne, R. Fagan, S. Hinder, D. E. McCormack, and S. C. Pillai, *RSC Adv.* **6**, 95232 (2016).
- [43] N. Wetchakun, B. Incessungvorn, K. Wetchakun, and S. Phanichphant, *Mater. Lett.* **82**, 195 (2012).
- [44] T. B. Ghosh, S. Dhabal, and A. K. Datta, *J. Appl. Phys.* **94**, 4577 (2003).
- [45] N. Satoh, T. Nakashima, and K. Yamamoto, *Sci. Rep.* **3**, 1959 (2013).
- [46] W. Humphrey, A. Dalke, and K. Schulten, *J. Mol. Graph.* **14**, 33 (1996).